Biochimica et Biophysica Acta 1798 (2010) 461–470

Contents lists available at ScienceDirect

Biochimica et Biophysica Acta

journal homepage: www.elsevier.com/locate/bbamem

# Structural and functional changes in a synthetic S5 segment of KvLQT1 channel as a result of a conserved amino acid substitution that occurs in LQT1 syndrome of human ☆

Richa Verma, Jimut Kanti Ghosh *

*Molecular and Structural Biology Division, Central Drug Research Institute, CSIR, Lucknow-226001, India*

ARTICLE INFO

*Article history:*
Received 12 August 2009
Received in revised form 9 December 2009
Accepted 17 December 2009
Available online 4 January 2010

*Keywords:*
Long QT syndrome
LQTS1 associated mutation
Voltage gated potassium channel
Cardiac voltage gated potassium channel—KvLQT1
Peptide–membrane interaction
Assembly of synthetic S5
Pore forming activity of S5 peptide in phospholipid vesicle

ABSTRACT

Mutations in various voltage gated cardiac ion channels are the cause of different forms of long QT syndrome (LQTS), which is an inherited arrhythmic disorder marked as a prolonged QT interval on electrocardiogram. Of these LQTS1 is associated with mutations in the gene encoding KCNQ1 (KvLQT1) channel. One responsible mutation, G269S, in the S5 segment of KvLQT1, that affects the proper expression and function of channel protein leads to LQTS1. Our objective was to study how G269S mutation interferes with the structure and function of a synthetic S5 segment of KvLQT1 channel. One wild type 22-residue peptide and another mutant peptide of the same length with G269S mutation, derived from the S5 segment were synthesized and labeled with fluorescent probes. The mutant peptide exhibited lower affinity towards phospholipid vesicles as compared to the wild type peptide and showed impaired assembly and localization onto the lipid vesicles as evidenced by membrane-binding, energy transfer and proteolytic cleavage experiments. Loss in the helical content of S5 mutant peptide in membrane-mimetic environments was observed. Furthermore, it was observed that G269S mutation significantly inhibited the ability of S5 peptide to permeabilize the lipid vesicles. The present studies show the basis of change in function of the selected S5 segment as a result of G269S mutation which is associated with LQT1 syndrome. We speculate that the structural and functional changes related to the glycine to serine amino acid substitution in the S5 segment may also influence the activity of the whole KvLQT1 channel.



## 1. Introduction

Voltage gated potassium channels (Kv) regulate the membrane potential of many excitable tissues. Kv channels are typically closed at the resting membrane potential, and open upon cell membrane depolarization. Kv channels bring about neuronal signaling, cardiovascular function, immune cell activation, muscle contraction and many other physiological processes [1–3]. Lack of proper expression and function of these channels cause severe disorders in humans such as episodic ataxia, long QT syndrome and epilepsy. The malfunction in Kv channels arises due to the mutations in the genes encoding that particular channel [4].

Long QT syndrome 1 (LQTS1), results from mutations in the gene encoding the KCNQ1 (KvLQT1) channel of the heart. These mutations lead to structural abnormalities in the KvLQT1 channels which cause sustained inward current or reduced outward current that prolongs the action potential and thus results in long QT interval which leads to LQT1 syndrome [5–8]. In cardiac myocytes, KvLQT1 tetramers combine with two KCNE1 (MinK) β-subunits to form functional Kv channel. These channels underlie $I_{KS}$, a slow delayed rectifier $K^+$ current that is involved in repolarization of the cardiac action potential and an important determinant of the QT interval of the electrocardiogram. Mutations that alter the function of either KvLQT1 or MinK subunit results in long QT1 syndrome [8–11].

To date, nearly 100 different KvLQT1 mutations have been reported as responsible for the cardiac long QT1 syndrome, characterized by prolonged QT interval, and sudden death [12]. It has been reported that a LQT1 syndrome is associated with the substitution of glycine to serine at position 269 of S5 segment. G269S mutation alters the structural and functional property of KvLQT1 channel subunits resulting in long QT1 syndrome which can lead to arrhythmias, ventricular fibrillation and cardiac arrest [13–18]. Interaction of these channel proteins with membranes and assembly there in are important issues related to their functions. However, the way the

*Abbreviations:* CD, circular dichroism; Fmoc, *N*-(9-fluorenyl)methoxycarbonyl; HPLC, high performance liquid chromatography; Kv, voltage gated potassium channels; LQTS, long QT syndrome; NBD, 7-nitrobenz-2-oxa-1,3-diazole; PBS, phosphate buffered saline (pH 7.4); PC, phosphatidylcholine; PG, phosphatidylglycerol; Rho, tetramethylrhodamine; LUVs, large unilamellar vesicles; TFE, trifluoroethanol; TM, transmembrane

☆ Central Drug Research Institute communication number of this manuscript is 7816.

* Corresponding author. Tel.: +91 522 2612411 18x4282; fax: +91 522 2623405.
*E-mail address:* jighosh@yahoo.com (J.K. Ghosh).

0005-2736/$ – see front matter © 2009 Elsevier B.V. All rights reserved.
doi:10.1016/j.bbamem.2009.12.014

LQTS mutations alter the membrane interaction and assembly of the protein is unknown. This work has been aimed to study the structural and functional changes associated with the LQT1 syndrome-causing mutation in some conserved segments of KvLQT1 channel. To look into the structural and functional alteration involved with the G269S point mutation in the concerned segment, a 22-residue peptide from S5 segment of KvLQT1 was synthesized; besides the mutant peptide of the same size with glycine to serine substitution at position 269, which causes the LQT syndrome was synthesized. The effect of glycine to serine substitution, on the secondary structure, assembly and membrane permeability of 22-residue segment was studied in detail.

## 2. Materials and methods

### 2.1. Materials

Rink amide MBHA resin (loading capacity: 0.4–0.8 mmol/g) and all the N-α Fmoc and necessary side-chain protected amino acids were purchased from Novabiochem, Laufelfingen, Switzerland. Coupling reagents for peptide synthesis like 1-hydroxybenzotriazole (HOBT), di-isopropylcarbodiimide (DIC), 1,1,3,3-tetramethyluronium tetrafluoroborate (TBTU) and N, N′-diisopropylethylamine (DIPEA) were purchased from St. Louis, MO, Sigma, USA. Dichloromethane (DCM), N, N′ dimethylformamide (DMF) and piperidine were of standard grades and procured from reputed local companies. Acetonitrile (HPLC grade) was procured from Merck, Mumbai India while trifluoroacetic acid (TFA), trifluoroethanol (TFE) and sodium dodecyl sulfate (SDS) were purchased from Sigma. Egg phosphatidylcholine (PC) and egg phosphatidylglycerol (PG) were obtained from Northern Lipids Inc., Burnaby BC V5J5J1 Canada. 3,3′-dipropylthiadicarbocyanine iodide (diS-$C_3$-5), NBD-fluoride (4-fluoro-7-nitrobenz-2-oxa-1, 3-diazole) and tetramethylrhodamine succinimidyl ester were procured from Molecular probes, Eugene, OR. The other reagents employed in this study were of analytical grade and procured locally; buffers were prepared in milli Q water ($USF^{ELGA}$).

### 2.2. Peptide synthesis, fluorescent labeling and purification

The peptide was synthesized manually on solid phase. Stepwise solid phase synthesis was carried out on rink amide MBHA resin (0.15 mmol) utilizing the standard Fmoc chemistry, employing DIC/HOBT or TBTU/HOBT/DIPEA coupling procedure [19,20]. De-protection of α-amino group and the coupling of amino acids were checked by Kaiser test [21] for primary amines. After the synthesis was over, each peptide was cleaved from the resin with simultaneous de-protection of side chains by treatment with a mixture of TFA/phenol/thioanisole/1,2-ethanedithiol/water (82.5:5:5:2.5:5 v/v) for 6–7 h. Labeling at the N-terminus of a peptide was achieved by a standard procedure reported earlier [22,23]. In brief, 15–20 mg of resin-bound peptide was treated with 25% piperidine (in DMF) to remove the Fmoc group from the N-terminal amino group. The resin was washed and dried. Then Fmoc de-protected resin-bound peptides were incubated with tetramethylrhodamine succinimidyl ester (2–3 equiv.) in dimethylformamide in the presence of 5% diisopropylethylamine for 48–72 h, which ultimately resulted in the formation of $N^{\alpha}$–Rho-peptides. Similarly, resin-bound peptides were treated with NBD-fluoride (2–3 equiv.) to obtain $N^{\alpha}$–NBD-peptides. After sufficient labeling, the resins were washed with DMF and DCM in order to remove the un-reacted probe. The peptides were cleaved from the resin as above and precipitated with dry ether. All the peptides were purified by RP-HPLC on an analytical Vydac C4 column using a linear gradient of 0–80% acetonitrile in 45 min with a flow rate of 0.6 ml/min. Both acetonitrile and water contained 0.05% TFA. The purified peptides were ~90% homogeneous as shown by HPLC. Each peptide was subjected to ES-MS analysis for the detection of molecular mass.

### 2.3. Preparation of large unilamellar vesicles (LUVs)

LUVs were prepared by a standard procedure [24,25] as follows. Dry lipids containing PC/PG (1:1 w/w) of required amounts were dissolved in $CHCl_3$/MeOH (2:1 v/v) in a small glass vial. Solvents were evaporated under a stream of nitrogen, which resulted in the formation of a thin film on the wall of the glass vessel. Also, films were dried overnight under vacuum to remove traces of solvents. The thin film was re-suspended in buffer at a concentration of 8.2 mg/ml by vortex mixing. The lipid dispersions were then sonicated in a bath-type sonicator (Laboratory Supplies Company, New York) for 10–20 min until it became transparent. The lipid concentration was determined by phosphorus estimation [26].

### 2.4. Circular dichroism (CD) experiments

The CD spectra of peptides were recorded in phosphate buffered saline (PBS, pH 7.4), 40% TFE and 1% SDS by utilizing a Jasco J-710 spectropolarimeter, Easton, MD, averaged over three scans, and baseline-corrected. Noise reduction was performed by using the manufacturer's software. The spectropolarimeter was calibrated routinely with 10-camphor sulphonic acid. The samples were scanned at room temperature (~30 °C) with the help of a capped quartz cuvette of 0.2 cm path length in the wavelength range of 250–195 nm. An average of 4–6 scans was taken for each sample with a scan speed of 20 nm/min and data interval of 0.5 nm for peptide concentration of 10–20 μM. The fractional helicities were calculated by the following formulae [27,28].

$$F_h = \frac{[\theta]_{222} - [\theta]^0{}_{222}}{[\theta]^{100}{}_{222} - [\theta]^0{}_{222}}$$

where $[\theta]_{222}$ was the experimentally observed mean residue ellipticity at 222 nm. The values for $[\theta]^{100}_{222}$ and $[\theta]^{0}_{222}$ that correspond to 100% and 0% helix contents were considered to have mean residue ellipticity values of −32,000 and −2000 respectively at 222 nm [28].

### 2.5. Membrane-binding experiments

The affinity of the peptide for phospholipid vesicles was determined by binding experiments as reported earlier [23,29–31]. In brief small unilamellar vesicles were added gradually to a freshly dissolved NBD-labeled peptide of ~0.30 μM concentration at room temperature. Fluorescence intensities of NBD-labeled peptides alone and after each addition of lipid vesicles were recorded on a Perkin Elmer spectrofluorimeter, model LS-50B MA, USA, with the excitation and emission wavelengths set at 467 and 528 nm respectively. The excitation and emission slits were fixed at 8 and 6 nm respectively. The contributions of lipid to any of the recorded signal were measured by titrating the unlabeled peptide (at the concentration of NBD-labeled peptide) with the same amount of lipid vesicles and were subtracted from the original fluorescence signal. The binding isotherms were analyzed by the following equation.

$$X_b^* = K_p^* C_f$$

where $X_b^*$ is defined as the molar ratio of bound peptide per 60% of the total lipid, assuming that the peptides were initially partitioned only over the outer leaflet of the LUVs as suggested by Beschiaschvili and Seelig [32]. $K_p^*$ represents the partition coefficient and $C_f$ indicates the concentration of the free peptide at equilibrium.

$X_b$ can be calculated by extrapolating the fluorescence signal $F_{infinity}$ (fluorescence signal when all the peptide molecules are bound to lipid) from a double-reciprocal plot of $F$ (peptide fluorescence in

the presence of lipid) versus $C_L$ (lipid concentration). Fraction of peptide bound ($f_b$) was determined by the following equation.

$$f_b = (F - F_0) / (F_{infinity} - F_0)$$

where $F$ is the fluorescence of the peptide when it is bound to lipid and $F_0$ is the fluorescence of the peptide in its unbound state. When $f_b$ is known, $C_f$ can easily be calculated for each concentration of the lipid. $K_p^*$ can easily be determined from the slope of the plot of $X_b^*$ and $C_f$. Partition coefficient of each of the peptides was determined as the average of the values obtained from two-three independent experiments as described previously [33,34].

### 2.6. Enzymatic cleavage experiments

In order to detect the location of the NBD-labeled peptide in its membrane-bound state, enzymatic cleavage experiments were performed as reported earlier [23,35]. In brief, PC/PG lipid vesicles were first added to the NBD-labeled peptide. When major portion of the peptide was bound to the lipid vesicles as detected by the saturation of the fluorescence level, proteinase-k (final concentration, 10.0 μg/ml) was added. In this experiment fluorescence of NBD-labeled peptide was recorded at 528 nm with respect to time (in sec) with excitation wavelength set at 467 nm. In the control experiment proteinase-k was first added to NBD-labeled peptide and then lipid vesicles were added. Percentage of a NBD-labeled peptide protected ($P_p$) from proteinase-k cleavage in its membrane-bound state was determined by the following equation:

$$P_p = \{(F_f - F_c) / (F_m - F_c)\} \times 100\%$$

where $F_f$ = Final fluorescence of the NBD-labeled peptide after proteinase-k treatment in its membrane-bound state; $F_c$ = Control fluorescence of proteinase-k-treated NBD-labeled peptide in PBS after addition of lipid vesicles; and $F_m$ = Maximum fluorescence of the membrane-bound NBD-labeled peptide before proteinase-k treatment.

### 2.7. Fluorescence resonance energy transfer experiment

Fluorescence energy transfer experiments were performed with excitation wavelength set at 467 nm and emission range of 500 to 600 nm. 0.3 μM of the NBD-labeled peptide was taken in a fluorimeter cuvette. 780 μM of the phospholipid vesicles was added to the NBD-labeled peptide to ensure that the peptides were bound to the membrane. Now Rho-labeled acceptor peptide was added to the donor peptide–lipid complex. Energy transfer from donor to acceptor was determined by subtracting the acceptor fluorescence in the presence of lipid and unlabeled donor from the fluorescence signal obtained in the presence of donor, acceptor and lipid vesicles.

The efficiency of energy transfer ($E$) was determined by the decrease in donor's fluorescence in the presence of the acceptor as reported earlier [23,36]. The percentage of energy transfer was calculated by the following equation.

$$E = \{(I_{D0} - I_{DA}) / I_{D0}\} \times 100$$

where $I_{D0}$ and $I_{DA}$ are the fluorescence intensities of the NBD-labeled donor peptide in the absence and presence of the Rho-labeled acceptor peptide respectively at the emission maxima of the donor after correcting the light scattering of the lipid vesicles and emission of the acceptor.

### 2.8. Calcein release from the calcein-entrapped lipid vesicles

Peptide-induced release of calcein from calcein-entrapped lipid vesicles was employed to detect the permeabilization of phospholipid membrane in the presence of S5 peptide and its mutant. Calcein-entrapped lipid vesicles were prepared with a self-quenching concentration (60 mM) of the dye in 10 mM HEPES at pH 7.4 as reported earlier [37,38]. Briefly, thin film of lipid (PC/PG) was re-suspended in calcein solution, vortexed for 1–2 min and then sonicated in a bath-type sonicator. The non-encapsulated calcein was removed from the liposome suspension by gel filtration using a sephadex G-50 column. Usually lipid vesicles are diluted to approximately 10 fold after passing through a G-50 column. The eluted calcein-entrapped vesicles were diluted further in the same buffer to a final lipid concentration of ~3.0 μM for the experiment. Peptide-induced release of calcein from the lipid vesicles was monitored by the increase in fluorescence due to the dilution of the dye from its self-quenched concentration. Fluorescence was monitored at room temperature with excitation and emission wavelengths fixed at 490 and 520 nm respectively. The peptide-induced release of calcein from the calcein-entrapped lipid vesicles was measured in terms of percentage of fluorescence recovery ($F_t$) as defined by [22,23]

$$F_t = [(I_t - I_0) / (I_f - I_0)] \times 100\%$$

where $I_t$ = the observed fluorescence after the addition of a peptide at time $t$, $I_0$ = the initial fluorescence of calcein-entrapped vesicles and $I_f$ = the increase in fluorescence observed after the addition of triton X-100 (0.1% final concentration) to the dye-entrapped vesicle suspension.

## 3. Results

### 3.1. Design and synthesis of peptides derived from conserved S5 segment of KvLQT1 potassium channel

The multiple sequence alignment of the S5 segment of KvLQT1 depicts the conservation of glycine residue at 269th position in the homologous channel proteins of the same family (Fig. 1A). In order to investigate the plausible effect of the disease (LQTS1) causing, G269S, mutation in the assembly and function of the concerned S5 segment, a 22-residue wild type and the mutant peptide corresponding to the amino acid region, 262–283 of S5 segment of KvLQT1 channel, were designed and synthesized (Fig. 1B). Fig. 1C represents the Schiffer and Edmundson wheel projections of the synthetic S5, which shows the arrangement of hydrophobic and hydrophilic amino acids revealing the amphipathic nature of the peptide and location of glycine in the hydrophobic face of the peptide.

### 3.2. G269S mutation impeded the S5 peptide-induced permeability of negatively charged PC/PG lipid vesicles

The S5 segment lines the pore of Kv channel along with S6 segment. In order to check the ability of S5 and its analogue to permeabilize the phospholipid membrane, release of calcein from calcein-entrapped lipid vesicles in the presence of these peptides was measured. As shown in Panel A of Fig. 2, the synthetic S5 peptide triggered the release of liposome-encapsulated calcein in a dose-dependent manner from PC/PG lipid vesicles as evidenced by the increase in calcein fluorescence following the addition of peptide. However, the S5 mutant peptide was significantly less efficient than the wild type S5 in releasing calcein from these (Fig. 2B) lipid vesicles indicating the abrogation of S5 peptide-induced membrane permeability following the glycine to serine substitution in this segment. It can be inferred that proper functioning of the selected S5 segment was averted by the disease causing G269S mutation in the synthetic peptide S5. Moreover, as shown in Fig. 2C, the plot of percentage of fluorescence recovery, a measure of peptide-induced membrane permeability, clearly indicated that the mutant was much less active than the wild type S5 in releasing liposome-encapsulated

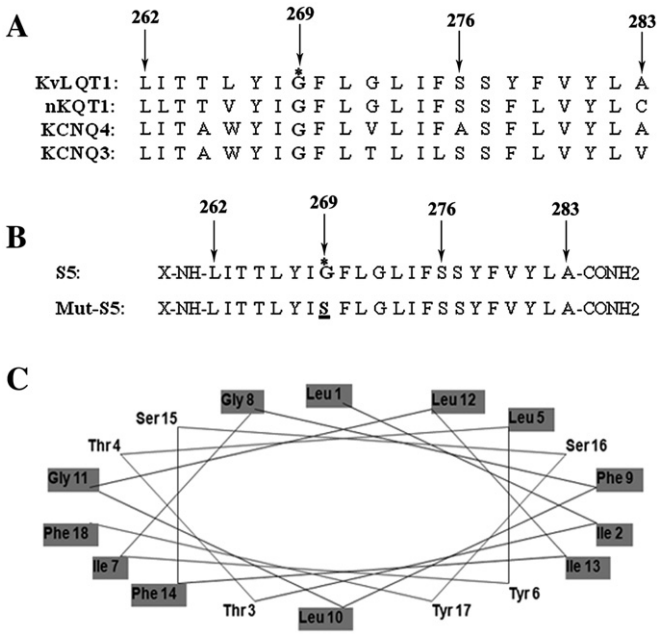


**Fig. 1.** Panel A, Sequence alignment of S5 segment (amino acids, 262–283) of human KvLQT1 with human KCNQ4, KCNQ3 and nKQT1of *Caenorhabditis elegans* homologous channels. Conserved G269 is marked in bold letter. The numbers above the amino acids indicate the corresponding amino acid numbers in the KvLQT1 protein. Panel B, Peptides designed from the S5 segment of KvLQT1 channel used in the study. Conserved G269 is marked in bold letter and mutated amino acid is marked as bold and underlined. (X = H, NBD and Rho). The amino acid marked with star in panels A and B indicates the amino acid that has been mutated. Panel C, Schiffer and Edmundson wheel projections of first 18 amino acids of S5 generated by Gene Runner program. Hydrophobic amino acids are marked as bold and shaded while hydrophilic amino acids are in regular characters.

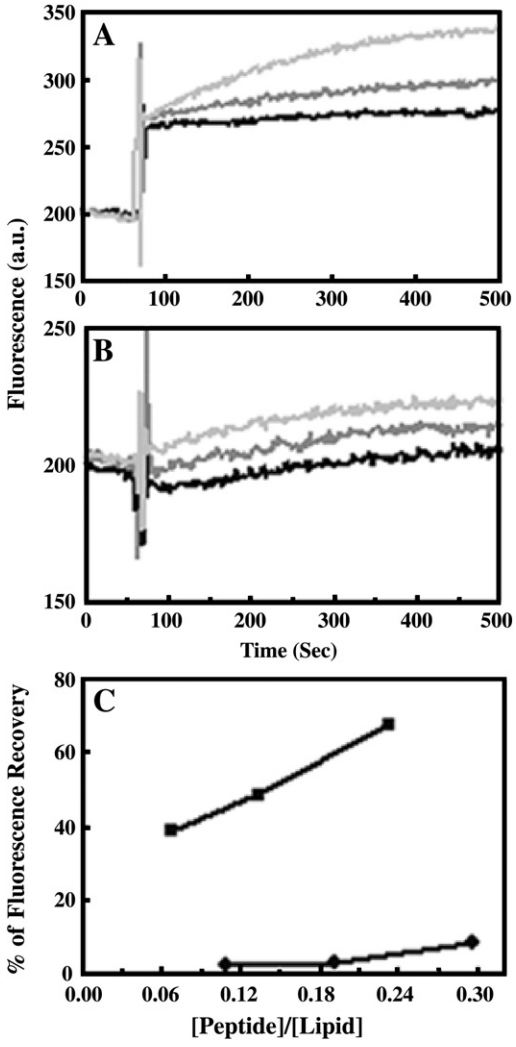


**Fig. 2.** Detection of calcein release induced by S5 and G269S mutant S5 peptide from the PC/PG lipid vesicles entrapped with calcein by recording its fluorescence. Panels A and B show the profiles of calcein release induced by increasing concentrations of S5 and Mut-S5 respectively as measured by the increase in calcein fluorescence with respect to time from calcein-entrapped PC/PG lipid vesicles (3.0 μM). Black line, gray line and light gray line are 0.2, 0.4 and 0.7 μM peptides of S5 in panel A and 0.3, 0.6 and 0.9 μM of Mut-S5 in panel B. Panel C depicts the relative membrane permeability of the S5 wild and mutant peptides in PC/PG lipid vesicles as shown by the plots of percentage of fluorescence recovery with respect to peptide to lipid molar ratio. Symbols: closed squares, S5 and closed circles, Mut-S5.

calcein in PC/PG lipid vesicles. Considering the fact that human cardiac cell membrane contains both zwitterionic as well as negatively charged phospholipids [39,40]; lipid vesicles, prepared with zwitterionic PC and negatively charged PG, were used in this study as a negatively charged model membrane. Furthermore, fluorescent labeled S5 peptide also induced appreciable calcein release (~90% to its unlabeled version) from PC/PG lipid vesicles suggesting that labeling of the peptide did not alter its activity.

### *3.3. G269S mutation influenced the membrane-binding property of synthetic S5 peptide*

To further examine the basis of impairment of membrane permeation by S5 mutant peptide in PC/PG lipid vesicles as compared to its wild type, the interaction of both peptides to PC/PG lipid vesicles was studied in detail. To detect the binding of S5 and its mutant to phospholipid vesicles, the peptides were labeled by fluorescent probe NBD. The sensitivity of the NBD probe to the dielectric constant of the medium has been exploited extensively to detect the binding of the NBD-labeled peptide to membrane [34,41–43].

Fluorescence emission spectra of NBD-labeled S5 and Mut-S5 were recorded in aqueous buffer and in the presence of PC/PG lipid vesicles. The fluorescence spectra of wild type and mutant peptides exhibited broad emission maxima around 543 ± 1 nm in phosphate buffer indicating the location of the NBD probe, attached to the N-terminal of the peptides in the hydrophilic environment [43]. However, in the presence of PC/PG (1:1, w/w) phospholipid vesicle fluorescence spectra of the NBD-labeled S5 and mutant peptide exhibited a blue shift of emission maxima concomitant with significant increase in fluorescence (Fig. 3). These shifts of emission maxima towards the shorter wavelength with increased fluorescence indicated the relocation of the probe in the hydrophobic environment due to binding of the peptides to phospholipid vesicles. Wild type S5 exhibited an emission maximum of 527 ± 1 nm in the presence of PC/PG lipid vesicles, which is shorter than the emission maximum of 533 nm, characteristic of the location of the NBD probe on the surface of membrane [44]. This emission maximum further suggested that the N-terminal of S5 was to some extent inserted in the bilayer of the PC/PG lipid vesicles. However, the NBD-labeled S5 mutant peptide displayed an emission maximum around 531–532 nm in the presence of PC/PG lipid vesicles suggesting that its N-terminal was most likely located on the surface of the membrane.

These results clearly demonstrated that though both wild type and the mutant peptides derived from S5 segment of KvLQT1 channel bound to PC/PG lipid vesicles, glycine to serine amino acid substitution disturbed the binding property and localization of wild type peptide onto the lipid vesicles.

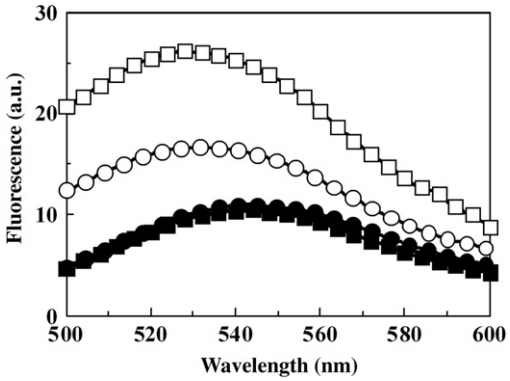


**Fig. 3.** Detection of binding of NBD-labeled-S5 and -G269S mutant peptide to lipid vesicles by recording fluorescence of these labeled peptides in PBS in the absence and in the presence of PC/PG vesicles. Squares and circles represent S5 and Mut-S5 respectively. Closed symbols, 0.3 μM NBD-labeled-S5 and its mutant peptide in PBS; open symbols, NBD-labeled peptides in the presence of 780 μM PC/PG lipid vesicles.

### *3.4. G269S mutation decreased the affinity of S5 peptide towards PC/PG lipid vesicles*

The affinity of S5 and its mutant to the PC/PG vesicles was determined by the binding experiments utilizing their NBD-labeled analogues and LUVs. Fluorescence signal of the NBD-labeled peptide as a result of its binding to the phospholipid membrane was plotted with respect to lipid/peptide molar ratio. Fig. 4A depicts the binding curve for S5 and Mut-S5 peptides in PC/PG lipid vesicles. Both plots indicate a gradual increase in fluorescence with increase in lipid concentration indicating a progressive binding of the NBD-labeled peptide molecules to the lipid vesicles. Binding isotherms were generated by plotting $X_b^*$ with respect to $C_f$ as has been described in the Materials and methods section. Partition coefficients of the NBD-labeled peptides to the phospholipid vesicles were estimated from the slope of the binding isotherms after extrapolating to zero. NBD-labeled S5 exhibited an appreciable affinity for PC/PG lipid vesicles as indicated (Fig. 4B) by its partition coefficient of $3.8\ (\pm 0.1)\times 10^4\ M^{-1}$, very similar to that of the surface-active peptides, derived from antimicrobial peptides, bacterial toxins and viral fusion proteins [22,23,45,46]. The estimated partition coefficient for the mutant peptide was $0.26\ (\pm 0.1)\times 10^4\ M^{-1}$ in the same kind of lipid vesicles. The binding isotherms of NBD-labeled Mut-S5 peptide in PC/PG (Fig. 4C) vesicles were linear in nature, suggesting that the binding of the mutant peptide to the phospholipid vesicles was a simple adhesion process and not associated with the formation of large aggregates there in PC/PG lipid vesicles.

However, the binding isotherm of NBD-labeled S5 in PC/PG vesicles (Fig. 4B) bent downward appreciably and deviated from linearity. As suggested earlier, this kind of curve indicates the co-operativity in binding of the peptide molecules to membrane [22,34,45]. The data indicated that the synthetic S5 segment formed large aggregates in lipid vesicles like pore-forming peptides, pardaxin and alamethicin [22,45]. Furthermore, these binding isotherms revealed that G269S mutation inhibited the wild type NBD-labeled S5 to form large aggregates in PC/PG lipid vesicles.

### *3.5. G269S mutation caused an easy cleavage of NBD-labeled S5 peptide by proteinase-k in its membrane-bound state*

To further examine the effect of replacement of glycine at 269 position by serine on the localization of the peptides onto the membrane, proteolytic cleavage experiments were performed with NBD-labeled peptides [23,36].

The basis of this experiment is that NBD-labeled peptides, bound onto the membrane surface, are easily cleaved by a proteolytic

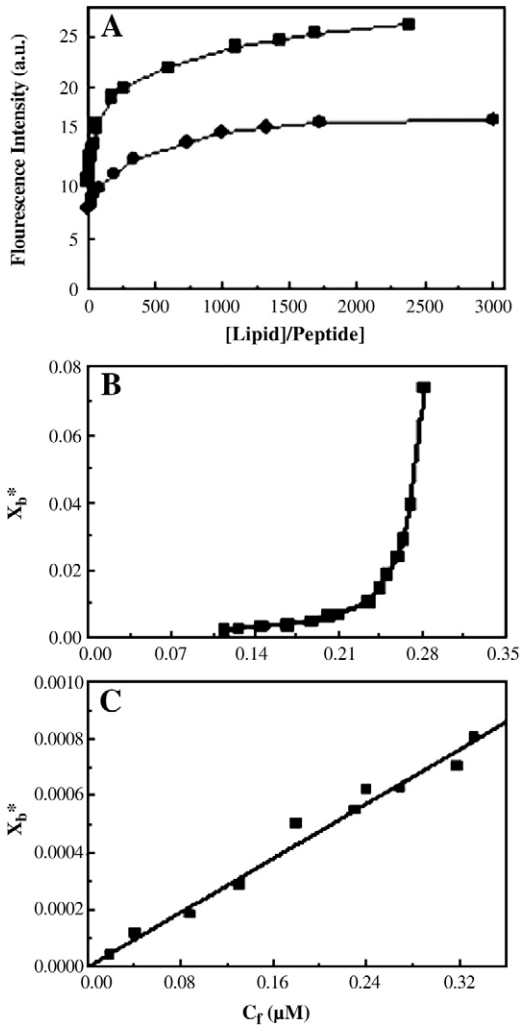


**Fig. 4.** Determination of the affinity of NBD-labeled-S5 and -G269S mutant peptide (0.3 μM) to phospholipid vesicles as detected by titration with PC/PG lipid vesicles. Fluorescence intensities of these labeled peptides were recorded in the absence and presence of varying amounts of lipid vesicles in PBS as described in the Materials and methods section. Panel A, Binding curve of S5 and Mut-S5 in PC/PG lipid vesicles. Panel B, Binding isotherm of S5 in PC/PG lipid vesicles. Panel C, Binding isotherm of Mut-S5 in PC/PG lipid vesicles. Symbols: In panel A, squares and circles represent S5 and Mut-S5; in panel B squares represent S5 and in panel C squares represent Mut-S5.

enzyme like proteinase-k, which can be monitored by the decrease in NBD-fluorescence from the characteristic membrane-bound level. On the other hand, a membrane-inserted peptide will not be accessible to proteinase-k and therefore the NBD-fluorescence will not decrease. Profile 'a' of panel A in Fig. 5 describes the proteolytic cleavage experiment with NBD-labeled wild type S5 in PC/PG lipid vesicles. At time point 1 NBD-labeled S5 was added to the buffer followed by the addition of PC/PG lipid vesicles at time point 2. The addition of lipid vesicles resulted in an increase in NBD-fluorescence due to binding of the peptide to the lipid vesicles.

At time point 3 when NBD-fluorescence has reached the plateau, indicating a saturation of binding of the labeled peptide to the membrane, proteinase-k was added. The addition of proteinase-k resulted in much less decrease in NBD-fluorescence level as compared to its maximum membrane-bound level before proteinase-k treatment. The percentage membrane-bound NBD-S5 peptide protected from proteinase-k cleavage was ~70% as per the equation depicted in the Materials and methods section of concerned portion. The result indicated that NBD-S5 appreciably protected itself from the digestion by proteolytic enzyme. No further decrease in the fluorescence was

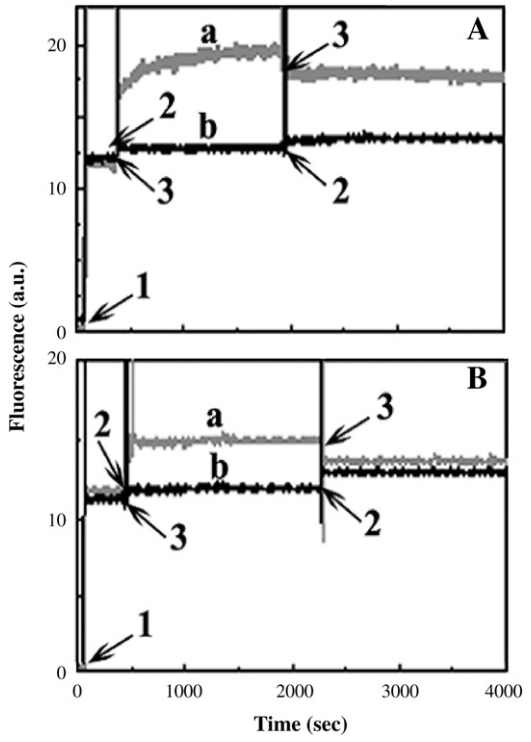


**Fig. 5.** Detection of the localization of NBD-labeled-S5 peptide and its analogue in their membrane-bound state by recording the fluorescence profiles of these labeled peptides with respect to time (s) in different experimental conditions. Panel A, S5 and panel B, Mut-S5. In trace a (gray line), 780 μM PC/PG lipid vesicles were added to 0.3 μM NBD-labeled S5 and G269S mutant peptide and then proteinase-k (10.0 μg/ml, final concentration) was added to membrane-bound peptide. In trace b (black line), proteinase-k was first added to the NBD-labeled peptides prior to the addition of lipid vesicles. Trace b (black line) is control. 1, 2, and 3 indicate the addition of peptide, lipid vesicles and proteinase-k respectively.

observed even after the incubation of ~2000 s. This result indicates that at least a part of the peptide was hidden inside the lipid bilayer and hence not cleaved even after a long incubation. A control experiment (profile 'b') was performed in order to check the cleavage of the peptide when it was not bound to phospholipid vesicles. Proteinase-k was added to the NBD-labeled peptide, incubated for sufficient time and then lipid vesicles were added. In this case addition of lipid vesicles resulted only in a small increase of NBD-fluorescence (compared to the previous experiment when vesicles were added to NBD-S5 before proteinase-k treatment) indicating that the peptides were cleaved by the enzyme and therefore unable to bind to the membrane.

Similar experiments were carried out with NBD-labeled S5 mutant peptide. For example, 'a' in panel B depicts the experimental profile of NBD-Mut-S5. In contrast to the wild type peptide, NBD-Mut-S5 was easily cleaved by proteinase-k in its membrane-bound state as evident from the sharp decrease in NBD-fluorescence after the addition of proteinase-k. The corresponding control experiment (profile 'b' of panel B) suggested that the mutant peptide was also cleaved easily when it was not bound to the membrane. As per the equation employed for determination of percentage of protection for a NBD-labeled peptide against proteinase-k cleavage in its membrane-bound state, the NBD-labeled mutant peptide was only ~30% protected as compared to 70% for NBD-S5.

These results suggest that the S5 wild type and mutant peptides were cleaved easily in aqueous buffer by proteinase-k. However, only the S5 wild type peptide resisted the proteolytic digestion after binding to PC/PG lipid vesicles probably due to its insertion into the lipid bilayer. Thus the data suggested that G269S mutation decreased the stability of S5 peptide in PC/PG lipid vesicles leading to early cleavage by proteinase-k.

### *3.6. G269S mutant S5 peptide exhibited significantly reduced helical structure in membrane-mimetic environments*

Circular dichroism studies were employed in order to determine the secondary structure of these peptides in aqueous and membrane-mimetic environments [47]. Secondary structures were determined in aqueous phosphate buffer saline (PBS), and in membrane-mimetic environments like SDS micelles and 40% TFE in water with the help of mean residual ellipticity values at 222 nm. Fig. 6 depicts the circular dichroism studies on these peptides in different environments. The two peptides exhibited mostly random coil structure in PBS, so not presented. The estimated helical structure as per the mean residual ellipticity value at 222 nm of the CD spectra of S5 and Mut-S5 were 53%, 5.7% in 1% SDS and 57.7%, 12% in 40% TFE in water (Table 1).

### *3.7. G269S mutation inhibited the self-assembly of S5 peptide in phospholipid vesicles*

Proper assembly of S5 peptide is a prerequisite for exhibiting its pore-forming activity. In order to evaluate any possible role of this conserved glycine at 269 position in the assembly of S5 segment in membrane, fluorescence energy transfer experiments were carried out in the presence of phospholipid vesicles. In order to perform the energy transfer experiments, both the wild type S5 and its mutant were labeled by fluorescence energy donor NBD and energy acceptor rhodamine. These two probes fulfill the spectroscopic criteria of fluorescence resonance energy transfer when they are in close proximity. Therefore, the assembly of a peptide can be determined with the help of energy transfer experiment between its NBD- and rhodamine-labeled analogues.

Panel A of Fig. 7 shows the fluorescence spectra of peptide energy transfer experiments between NBD-S5 peptide and Rho-labeled S5 in PC/PG lipid vesicles. Fluorescence spectra of NBD-S5 in PC/PG vesicles were recorded in the presence of increasing amounts of Rho-S5. As

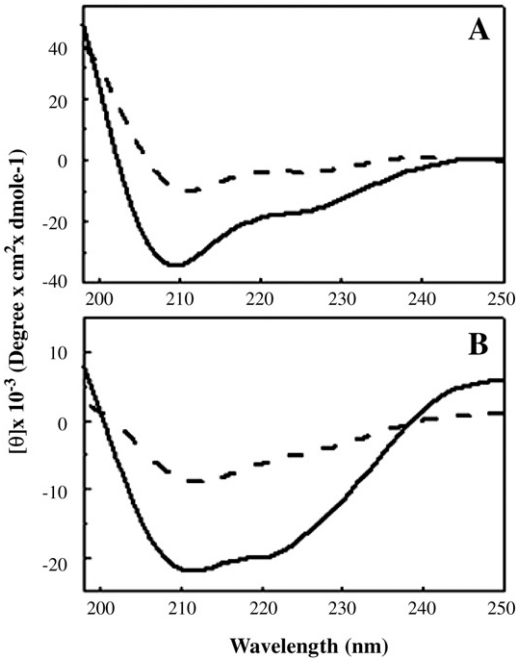


**Fig. 6.** Determination of secondary structures of S5 and G269S mutant peptides by recording their CD spectra in 1% SDS micelles (A) and in 40% TFE (B) in water. Symbols: solid line, S5; dash, Mut-S5. The concentrations of S5 and Mut-S5 were 23.9 and 23.6 μM respectively.

**Table 1**
The mean residue ellipticity values of S5 and its mutant peptide at 222 nm in different environments and corresponding percentage helicity.

| Peptide | MRE in 1% SDS | MRE in 40% TFE | %Helicity in 1% SDS | %Helicity in 40% TFE |
|---|---|---|---|---|
| S5 | 17,900 | 19,300 | 53.0 | 57.7 |
| Mut-S5 | 3700 | 5600 | 5.7 | 12.0 |

shown in panel A of Fig. 7, the addition of energy acceptor, Rho-S5 to the membrane-bound donor NBD-S5 resulted in an appreciable decrease in NBD-fluorescence concomitant with the increase in rhodamine fluorescence. This observation suggested that S5 peptide self-assembled in PC/PG lipid vesicles.

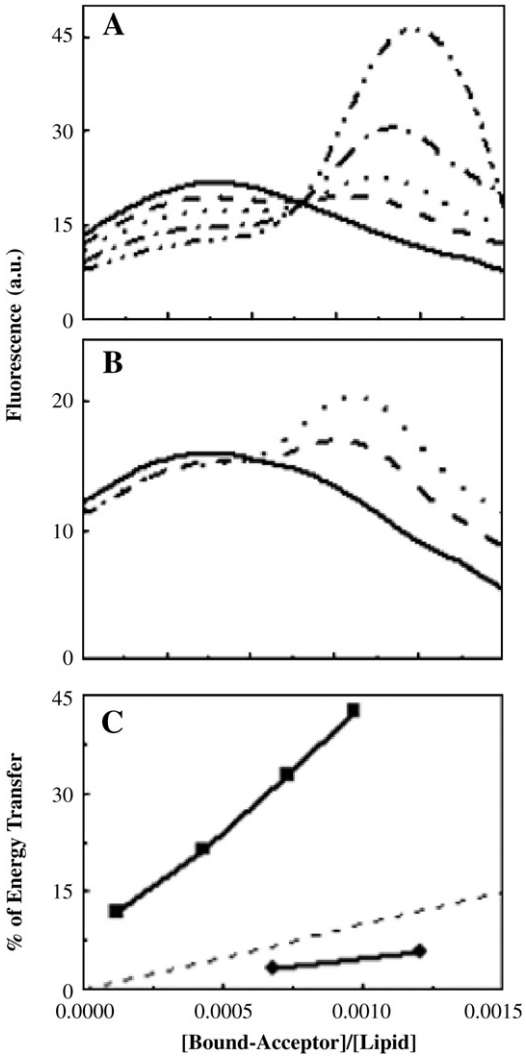


**Fig. 7.** Self-assembly of S5 and G269S mutant peptide by studying the fluorescence energy transfer experiments with NBD-labeled donor and Rho-labeled acceptor peptides in PC/PG lipid vesicles. The spectra were recorded with the donor peptide alone and in the presence of varying concentrations of acceptor peptide with excitation wavelength set at 467 nm. Panel A, the spectra of NBD-S5 (0.3 μM) in the presence of 780 μM of PC/PG (1:1) lipid vesicles alone (solid line) with various concentrations of Rho-S5: dash, 0.21 μM; dot, 0.4 μM; short dash dot, 0.62 μM short dash dot dot, 0.85 μM. Panel B, the spectra of NBD-Mut-S5 (0.3 μM) in the presence of 780 μM of PC/PG (1:1) lipid vesicles alone (solid line) with various concentrations of Rho-Mut-S5: dash, 0.45 μM; dot, 0.88 μM. Panel C, the plot showing percentage experimental energy transfers of different pairs and theoretical energy transfer corresponding to randomly distributed donor and acceptor with respect to the molar ratio of bound acceptor and lipid. Symbols: squares, S5; circles, Mut-S5.

Panel B of Fig. 7 depicts the results of energy transfer experiments between NBD-Mut-S5 and Rho-Mut-S5 peptide in PC/PG vesicles. In contrast to the wild type peptide, fluorescence of the donor peptide decreased only a little as a result of the addition of the acceptor peptide Rho-Mut-S5. These results clearly suggested that the Mut-S5 peptide did not self-assemble significantly in PC/PG vesicles and therefore, no appreciable decrease in fluorescence of NBD-Mut-S5 was observed when Rho-Mut-S5 was added to the former's membrane-bound state.

In order to confirm that the observed energy transfer was due to the assembly of the peptides, the percentages of energy transfer with different pairs of energy donor and acceptor were compared with that of the randomly distributed energy donor and acceptor as described earlier [36,48]. Panel C of Fig. 7 shows such plots, which clearly indicate that the energy transfer efficiencies of NBD-S5and Rho-S5 in PC/PG vesicles were much above the random distribution level. However, energy transfer efficiency of Mut-S5 pair was close to the random distribution level.

## 4. Discussion

The data presented here indicate that the changes reported in the functional property of KvLQT1 channel [18,49] owing to G269S mutation can produce significant alterations in the functional activity of the synthetic, 22-residue, S5 peptide which is associated with its binding, secondary structure and assembly in phospholipid membrane. The conserved nature of glycine at position 269 in the homologous proteins reflects the noteworthy importance of this residue in the structure and/or function of the S5 segment of KvLQT1 channel protein.

The synthetic S5 segment of KvLQT1 induced the release of calcein from calcein-entrapped PC/PG lipid vesicles much more efficiently than its mutant, Mut-S5, of the same size (Fig. 2). Binding experiments by employing the NBD-labeled peptides indicated that S5 and its mutant peptides bound onto the PC/PG lipid vesicles (Fig. 3). However, the mutant peptide with G269S mutation showed a reduced affinity than S5 towards the PC/PG lipid vesicles (Fig. 4), reflecting that G269S mutation in S5 influenced its binding property in lipid vesicles.

Proteolytic cleavage experiments (Fig. 5) with NBD-labeled S5 wild type and mutant peptide indicated that the wild type S5 peptide was probably inserted into the lipid bilayer while the mutant peptide resided on the surface of the lipid vesicles and hence was cleaved promptly by the enzyme. These results indicated the role of conserved glycine in localization of this synthetic S5 peptide in the PC/PG lipid vesicles. The results of the proteolytic cleavage experiments were supported by the characteristic emission spectra of NBD-labeled wild type and mutant peptide in negatively charged lipid vesicles. The observed emission maximum of around $527 \pm 1$ nm exhibited by NBD-S5 in PC/PG lipid vesicles (Fig. 3) was much shorter than that observed for NBD probe (533 nm) located on the surface of the membrane [44]. Whereas, emission maximum exhibited by NBD-Mut-S5 in PC/PG lipid vesicles (531–532 nm) was close to the characteristic emission maximum of the probe, located onto the membrane surface. Earlier reports also indicated that various disease causing mutations due to amino acid substitution by polar residues caused a transverse shift in the transmembrane helices that altered the inserted position and stability of the helices in the membrane [50–54].

Energy transfer experiments (Fig. 7) clearly demonstrated that only the wild type S5 but not its mutant could self-assemble in PC/PG lipid vesicles. This observation indicates that the substitution of the highly conserved glycine at 269 position with serine abrogated the self-assembly of S5 peptide defining a probable structural basis for its malfunctioning. Furthermore, these results were supported by the binding experiment data, which suggested that only the wild type S5 peptide formed large aggregates in negatively charged PC/PG vesicles

like other pore-forming peptides, which include pardaxin and alamethicin [22,45]. Significant change in secondary structure of S5 peptide (Fig. 6) in membrane-mimetic detergent was also observed as a result of replacement of glycine by serine at 269 positions. Along with the membrane-binding and the energy transfer results, it appeared that although S5 and G269S mutant S5 peptide bound to the lipid vesicles, only S5 peptide could self-assemble and formed large aggregates there. Due to G269S mutation the mutant peptide molecules might be distributed randomly in the lipid vesicles and were unable to self-assemble in the PC/PG lipid vesicles. A glycine to serine substitution (G389S) in the anchor region of *Yersinia* adhesin A (YadA), which is a trimeric pore-forming autotransporter adhesin of enteric yersiniae has been reported to abrogate its autotransporter function. The substitution of this conserved glycine by serine completely shifted the trimeric assembly of the autotransporter into monomer and subsequently a reduced protein expression, decreased stability and increased degradation of YadA by the periplasmic protease were observed [55,56].

Taken together, the results of the present study reflect that the mutant peptide bound to phospholipid vesicles yet assembled weakly in the lipid vesicles and did not induce any appreciable leakage in the PC/PG lipid vesicles. Probably, the impairment of assembly and function of this S5 transmembrane segment as a result of substitution of glycine to serine may influence the activity of the KvLQT1 and could be a possible way of how the proper functioning of the channel is affected by this substitution.

Peptide-induced pore-formation has been frequently detected by peptide-induced calcein release from the calcein-entrapped lipid vesicles [24,34,57–60]. The release of calcein from calcein-entrapped lipid vesicles in the presence of pardaxin, [24,57], melittin [58] and alamethicin [61] has been implicated to the pore-forming activity of the peptides. This is in contrast to the study of Benachir and Lafleur [62] which suggested that calcein release induced by melittin from calcein-entrapped 1-palmitoyl-2-oleoylphosphatidylcholine (POPC) vesicles was due to co-operative membrane perturbation rather than formation of pores. Similarly, magainin was proposed to permeabilize POPC lipid vesicles as evidenced by peptide-induced calcein release by perturbing the lipid bilayer without forming pores [63]. However, in the present study the S5 peptide self-assembled, inserted into the negatively charged lipid vesicles and also induced the release of calcein from these vesicles. These properties of S5 peptide match with the properties of other pore-forming peptides. Moreover, it is to be mentioned that while studying magainin–POPC membrane interaction, no aggregation or insertion of the peptide was observed [63]. Thus it is more likely that wild type S5 peptide-induced calcein release from calcein-entrapped PC/PG lipid vesicles was associated with pore-formation therein and G269S mutation impaired this activity.

Literature indicates that a glycine can modulate assembly of TM segments and is a common amino acid in the packing interface of TM helices [64]. It is also a key amino acid in van der Waals mediated packing of TM helices as its small size allows close interaction of TM segments. Glycine or an apolar to polar amino acid mutation could give rise to non-native to H-bond induced misfolding of a protein or alteration of helical packing through steric hindrance [65]. Indeed, eighty or so membrane proteins listed in the database of protein misfolding associated human diseases; approximately 50% of these contain apolar to polar amino acid substitutions in a TM helix. A number of glycine to serine amino acid substitutions in channel proteins have been reported that are involved with diseases. A missense mutation in KCNQ4, G285S is reported to be involved in dominant deafness [66]. A single-nucleotide-polymorphism (SNP) in the KCNE1 gene leading to glycine substitution for serine at amino acid position, 38, has been reported to be associated with increased atrial fibrillation incidence [67–70]. A G156S mutation in highly conserved G156 of an inward rectifying $K^+$ channel GIRK2, results in weaver phenotype that is inherited as an autosomal recessive disorder and results in severe ataxia and cell loss in substantia nigra [71].

Structural studies on membrane proteins are often difficult due to their high hydrophobicity, tendency to aggregate and problems in purifying in their native states. Consequently, several studies have been carried out recently with the synthetic peptides derived from the potentially crucial structural and functional segments of these membrane proteins [72–75]. It has been demonstrated that these peptides can assume functional assembly like their parent membrane proteins even in detergent micelles [75]. These studies have led to important conclusions related to the structural and functional contributions of the selected segments to the whole proteins and also provided valuable idea about the structure of the concerned proteins. The studies on synthetic peptides from CFTR channel [76,77], divalent metal ion transporter [72], sodium pump γ subunit [78] showed the effect of disease causing point mutation in the structure and assembly of these peptides and have been proposed to contribute in these diseases in vivo. Disease causing mutations at conserved glycine in the peptides derived from the gamma subunit of Na, K-ATPase and TM domain of Myelin protein zero, have been reported to abrogate their insertion and oligomerization in model membranes [78,79]. The present study on the effect of substitution of conserved glycine at 269 position by serine in a S5 peptide of KvLQT1 channel showed a significant loss of its secondary structure in membrane-mimetic environment, assembly and insertion property in model membrane. Thus this mutation in the S5 segment may interfere with the proper folding of the protein and impair its trafficking, which further could be relevant to the pathogenesis of LQT1 syndrome. However, how exactly the G269S mutation in KvLQT1 channel causes the pathogenesis in LQT1 syndrome remains to be determined.

In conclusion, the results presented here demonstrated the structural and functional changes in the selected 22-residue segment of KvLQT1 channel that occurred as a result of substitution of glycine at 269 position by serine, involved with LQT syndrome in human. G269S mutation produced alterations not only in affinity and stability but also in assembly of S5 peptide in the lipid vesicles. The studies of synthetic S5 and its mutant peptide reflected the importance of G269 in its membrane-assembly and function of S5 peptide. Proper assembly of any pore-forming or ion channel protein is an essential criterion for its functional activity. Therefore, in the context of structural and functional changes observed in the S5 segment as a result of G269S amino acid substitution, it is possible that the same amino acid substitution could affect the structural and functional properties of KvLQT1 channel. Considering the fact that glycine to serine substitution in several membrane–proteins is associated with diseases, the present study also provides valuable information on their possible structural and functional alteration as a result of this amino acid substitution.

## Acknowledgements

This work was supported by a Central Drug Research Institute (CDRI) in house project no. MLP 0007M. RV acknowledges the receipt of Senior Research Fellowship from CSIR, India. Dr. R. M. Srivastava and Mr. B. K. Pandey are thankfully acknowledged for modifying Figs. 4 and 1 respectively.

## References

[1] P. Delmas, D.A. Brown, Pathways modulating neural KCNQ/M (Kv7) potassium channels, Nat. Rev. Neurosci. 6 (2005) 850–862.
[2] J. Robbins, KCNQ potassium channels: physiology, pathophysiology, and pharmacology, Pharmacol. Ther. 90 (2001) 1–19.
[3] A. Felipe, R. Vicente, N. Villalonga, M. Roura-Ferrer, R. Martinez-Marmol, L. Sole, J.C. Ferreres, E. Condom, Potassium channels: new targets in cancer therapy, Cancer Detect. Prev. 30 (2006) 375–385.

[4] Q. Wang, M.E. Curran, I. Splawski, T.C. Burn, J.M. Millholland, T.J. VanRaay, J. Shen, K.W. Timothy, G.M. Vincent, T. de Jager, P.J. Schwartz, J.A. Toubin, A.J. Moss, D.L. Atkinson, G.M. Landes, T.D. Connors, M.T. Keating, Positional cloning of a novel potassium channel gene: KVLQT1 mutations cause cardiac arrhythmias, Nat. Genet. 12 (1996) 17–23.
[5] D.M. Roden, A.L. George Jr., P.B. Bennett, Recent advances in understanding the molecular mechanisms of the long QT syndrome, J. Cardiovasc. Electrophysiol. 6 (1995) 1023–1031.
[6] M.E. Curran, I. Splawski, K.W. Timothy, G.M. Vincent, E.D. Green, M.T. Keating, A molecular basis for cardiac arrhythmia: HERG mutations cause long QT syndrome, Cell 80 (1995) 795–803.
[7] M. Boutjdir, M. Restivo, Y. Wei, K. Stergiopoulos, N. el-Sherif, Early after-depolarization formation in cardiac myocytes: analysis of phase plane patterns, action potential, and membrane currents, J. Cardiovasc. Electrophysiol. 5 (1994) 609–620.
[8] T. Jespersen, M. Grunnet, S.P. Olesen, The KCNQ1 potassium channel: from gene to physiological function, Physiology (Bethesda) 20 (2005) 408–416.
[9] M. Schwake, T.J. Jentsch, T. Friedrich, A carboxy-terminal domain determines the subunit specificity of KCNQ K+ channel assembly, EMBO Rep. 4 (2003) 76–81.
[10] C.E. Chiang, D.M. Roden, The long QT syndromes: genetic basis and clinical implications, J. Am. Coll. Cardiol. 36 (2000) 1–12.
[11] E. Herbert, M. Trusz-Gluza, E. Moric, E. Smilowska-Dzielicka, U. Mazurek, T. Wilczok, KCNQ1 gene mutations and the respective genotype–phenotype correlations in the long QT syndrome, Med. Sci. Monit. 8 (2002) RA240–RA248.
[12] G. Loussouarn, I. Baro, D. Escande, KCNQ1 K+ channel-mediated cardiac channelopathies, Methods Mol. Biol. 337 (2006) 167–183.
[13] G.M. Vincent, K.W. Timothy, M. Leppert, M. Keating, The spectrum of symptoms and QT intervals in carriers of the gene for the long-QT syndrome, N. Engl. J. Med. 327 (1992) 846–852.
[14] G.M. Vincent, Hypothesis for the molecular physiology of the Romano–Ward long QT syndrome, J. Am. Coll. Cardiol. 20 (1992) 500–503.
[15] W. Creighton, R. Virmani, R. Kutys, A. Burke, Identification of novel missense mutations of cardiac ryanodine receptor gene in exercise-induced sudden death at autopsy, J. Mol. Diagn. 8 (2006) 62–67.
[16] M.J. Ackerman, D.J. Tester, C.J. Porter, Swimming, a gene-specific arrhythmogenic trigger for inherited long QT syndrome, Mayo Clin. Proc. 74 (1999) 1088–1094.
[17] M.J. Ackerman, D.J. Tester, C.J. Porter, W.D. Edwards, Molecular diagnosis of the inherited long-QT syndrome in a woman who died after near-drowning, N. Engl. J. Med. 341 (1999) 1121–1125.
[18] S. Chen, L. Zhang, R.M. Bryant, G.M. Vincent, M. Flippin, J.C. Lee, E. Brown, F. Zimmerman, R. Rozich, P. Szafranski, C. Oberti, R. Sterba, D. Marangi, P.J. Tchou, M.K. Chung, Q. Wang, KCNQ1 mutations in patients with a family history of lethal cardiac arrhythmias and sudden death, Clin. Genet. 63 (2003) 273–282.
[19] G.B. Fields, R.L. Noble, Solid phase peptide synthesis utilizing 9-fluorenylmethoxycarbonyl amino acids, Int. J. Pept. Protein Res. 35 (1990) 161–214.
[20] E. Bouchayer, C.I. Stassinopoulou, C. Tzougraki, D. Marion, P. Gans, NMR and CD conformational studies of the C-terminal 16-peptides of Pseudomonas aeruginosa c551 and Hydrogenobacter thermophilus c552 cytochromes, J. Pept. Res. 57 (2001) 39–47.
[21] E. Kaiser, R.L. Colescott, C.D. Bossinger, P.I. Cook, Color test for detection of free terminal amino groups in the solid-phase synthesis of peptides, Anal. Biochem. 34 (1970) 595–598.
[22] D. Rapaport, Y. Shai, Aggregation and organization of pardaxin in phospholipid membranes. A fluorescence energy transfer study, J. Biol. Chem. 267 (1992) 6502–6509.
[23] J.K. Ghosh, M. Ovadia, Y. Shai, A leucine zipper motif in the ectodomain of Sendai virus fusion protein assembles in solution and in membranes and specifically binds biologically-active peptides and the virus, Biochemistry 36 (1997) 15451–15462.
[24] Y. Shai, Y.R. Hadari, A. Finkels, pH-dependent pore formation properties of pardaxin analogues, J. Biol. Chem. 266 (1991) 22346–22354.
[25] J.K. Ghosh, Y. Shai, A peptide derived from a conserved domain of Sendai virus fusion protein inhibits virus–cell fusion. A plausible mode of action, J. Biol. Chem. 273 (1998) 7252–7259.
[26] G.R. Bartlett, Phosphorus assay in column chromatography, J. Biol. Chem. 234 (1959) 466–468.
[27] N. Greenfield, G.D. Fasman, Computed circular dichroism spectra for the evaluation of protein conformation, Biochemistry 8 (1969) 4108–4116.
[28] C.S. Wu, K. Ikeda, J.T. Yang, Ordered conformation of polypeptides and proteins in acidic dodecyl sulfate solution, Biochemistry 20 (1981) 566–570.
[29] D. Rapaport, Y. Shai, Interaction of fluorescently labeled pardaxin and its analogues with lipid bilayers, J. Biol. Chem. 266 (1991) 23769–23775.
[30] G. Schwarz, H. Gerke, V. Rizzo, S. Stankowski, Incorporation kinetics in a membrane, studied with the pore-forming peptide alamethicin, Biophys. J. 52 (1987) 685–692.
[31] G. Beschiaschvili, J. Seelig, Melittin binding to mixed phosphatidylglycerol/phosphatidylcholine membranes, Biochemistry 29 (1990) 52–58.
[32] G. Beschiaschvili, J. Seelig, Peptide binding to lipid bilayers. Binding isotherms and zeta-potential of a cyclic somatostatin analogue, Biochemistry 29 (1990) 10995–101000.
[33] S.P. Yadav, A. Ahmad, J.K. Ghosh, Addition of a small hydrophobic segment from the head region to an amphipathic leucine zipper like motif of E. coli toxin hemolysin E enhances the peptide-induced permeability of zwitterionic lipid vesicles, Biochim. Biophys. Acta 1768 (2007) 1574–1582.
[34] S.P. Yadav, B. Kundu, J.K. Ghosh, Identification and characterization of an amphipathic leucine zipper-like motif in Escherichia coli toxin hemolysin E. Plausible role in the assembly and membrane destabilization, J. Biol. Chem. 278 (2003) 51023–51034.
[35] E. Gazit, Y. Shai, Structural characterization, membrane interaction, and specific assembly within phospholipid membranes of hydrophobic segments from Bacillus thuringiensis var. israelensis cytolytic toxin, Biochemistry 32 (1993) 12363–12371.
[36] E. Gazit, Y. Shai, The assembly and organization of the alpha 5 and alpha 7 helices from the pore-forming domain of Bacillus thuringiensis delta-endotoxin. Relevance to a functional model, J. Biol. Chem. 270 (1995) 2571–2578.
[37] T.M. Allen, G. Cleland, Serum-induced leakage of liposome contents, Biochim. Biophys. Acta 597 (1980) 418–426.
[38] Y. Pouny, D. Rapaport, A. Mor, P. Nicolas, Y. Shai, Interaction of antimicrobial dermaseptin and its fluorescently labeled analogues with phospholipid membranes, Biochemistry 31 (1992) 12416–12423.
[39] B. Hamplova, V. Pelouch, O. Novakova, J. Skovranek, B. Hucin, F. Novak, Phospholipid composition of myocardium in children with normoxemic and hypoxemic congenital heart diseases, Physiol. Res. 53 (2004) 557–560.
[40] G. Rocquelin, L. Guenot, P.O. Astorg, M. David, Phospholipid content and fatty acid composition of human heart, Lipids 24 (1989) 775–780.
[41] R.A. Kenner, A.A. Aboderin, A new fluorescent probe for protein and nucleoprotein conformation. Binding of 7-(p-methoxybenzylamino)-4-nitrobenzoxadiazole to bovine trypsinogen and bacterial ribosomes, Biochemistry 10 (1971) 4433–4440.
[42] G. Bailin, J.R. Huang, Fluorescence properties of the Ca2+, Mg2(+)-ATPase protein of sarcoplasmic reticulum labeled with 7-chloro-4-nitrobenzo-2-oxa-1, 3-diazole, FEBS Lett. 259 (1990) 254–256.
[43] K. Rajarathnam, J. Hochman, M. Schindler, S. Ferguson-Miller, Synthesis, location, and lateral mobility of fluorescently labeled ubiquinone 10 in mitochondrial and artificial membranes, Biochemistry 28 (1989) 3168–3176.
[44] A. Chattopadhyay, E. London, Parallax method for direct measurement of membrane penetration depth utilizing fluorescence quenching by spin-labeled phospholipids, Biochemistry 26 (1987) 39–45.
[45] V. Rizzo, S. Stankowski, G. Schwarz, Alamethicin incorporation in lipid bilayers: a thermodynamic study, Biochemistry 26 (1987) 2751–2759.
[46] E. Gazit, A. Boman, H.G. Boman, Y. Shai, Interaction of the mammalian antibacterial peptide cecropin P1 with phospholipid vesicles, Biochemistry 34 (1995) 11479–11488.
[47] S.P. Yadav, A. Ahmad, B.K. Pandey, R. Verma, J.K. Ghosh, Inhibition of lytic activity of Escherichia coli toxin hemolysin E against human red blood cells by a leucine zipper peptide and understanding the underlying mechanism, Biochemistry 47 (2008) 2134–2142.
[48] B.K. Fung, L. Stryer, Surface density determination in membranes by fluorescence energy transfer, Biochemistry 17 (1978) 5241–5248.
[49] W. Shimizu, T. Noda, H. Takaki, N. Nagaya, K. Satomi, T. Kurita, K. Suyama, N. Aihara, K. Sunagawa, S. Echigo, Y. Miyamoto, Y. Yoshimasa, K. Nakamura, T. Ohe, J.A. Towbin, S.G. Priori, S. Kamakura, Diagnostic value of epinephrine test for genotyping LQT1, LQT2, and LQT3 forms of congenital long QT syndrome, Heart Rhythm 1 (2004) 276–283.
[50] C.N. Chin, G. von Heijne, Charge pair interactions in a model transmembrane helix in the ER membrane, J. Mol. Biol. 303 (2000) 1–5.
[51] H. Borochov, M. Shinitzky, Vertical displacement of membrane proteins mediated by changes in microviscosity, Proc. Natl. Acad. Sci. U. S. A. 73 (1976) 4526–4530.
[52] M. Monne, I. Nilsson, M. Johansson, N. Elmhed, G. von Heijne, Positively and negatively charged residues have different effects on the position in the membrane of a model transmembrane helix, J. Mol. Biol. 284 (1998) 1177–1183.
[53] C. Landolt-Marticorena, K.A. Williams, C.M. Deber, R.A. Reithmeier, Non-random distribution of amino acids in the transmembrane segments of human type I single span membrane proteins, J. Mol. Biol. 229 (1993) 602–608.
[54] G. Zhao, E. London, An amino acid "transmembrane tendency" scale that approaches the theoretical limit to accuracy for prediction of transmembrane helices: relationship to biological hydrophobicity, Protein Sci. 15 (2006) 1987–2001.
[55] U. Grosskinsky, M. Schutz, M. Fritz, Y. Schmid, M.C. Lamparter, P. Szczesny, A.N. Lupas, I.B. Autenrieth, D. Linke, A conserved glycine residue of trimeric autotransporter domains plays a key role in Yersinia adhesin A autotransport, J. Bacteriol. 189 (2007) 9011–9019.
[56] E. Hoiczyk, A. Roggenkamp, M. Reichenbecher, A. Lupas, J. Heesemann, Structure and sequence analysis of Yersinia YadA and Moraxella UspAs reveal a novel class of adhesins, EMBO J. 19 (2000) 5989–5999.
[57] Doron Rapaport, Ruth Peled, Shlomo Nir, Yechiel Shai, Reversible surface aggregation in pore formation by pardaxin, Biophys. J. 70 (1996) 2502–2512.
[58] Katsumi Matsuzaki, Shuji Yoneyama, Koichira Miyajima, Pore formation and translocation of melittin, Biophys. J. 73 (1997) 831–838.
[59] S. Kobayashi, Y. Hirakura, Katsumi Matsuzaki, Bacteria-selective synergism between the antimicrobial peptides alpha-helical magainin 2 and cyclic beta-sheet tachyplesin I: toward cocktail therapy, Biochemistry 40 (2001) 14330–14335.
[60] Takashi Katsu, Tomonori Imamura, Keiko Komagoe, Kazufumi Masuda, Tohru Mizushima, Simultaneous measurements of K+ and calcein release from liposomes and the determination of pore size formed in a membrane, Anal. Sci. 23 (2007) 517–522.
[61] S.H. Portlock, M.J. Clague, R.J. Cherry, Leakage of internal markers from eryhthrocytes and lipid vesicles included by melittin, gramicidinS and alamethicin, a comparative study, Biochim. Biophys. Acta 1030 (1990) 1–10.
[62] Toni Benachir, Michel Lafleur, Study of vesicle leakage induced by melittin, Biochim. Biophys. Acta 1235 (1995) 452–460.

[63] Torsten Wieprecht, Michael Beyermann, Joachim Seelig, Binding of antimicrobial magainin peptides to electrically neutral membranes: thermodynamics and structure, Biochemistry 38 (1999) 10377–10387.
[64] W.P. Russ, D.M. Engelman, The GxxxG motif: a framework for transmembrane helix–helix association, J. Mol. Biol. 296 (2000) 911–919.
[65] A.W. Partridge, A.G. Therien, C.M. Deber, Polar mutations in membrane proteins as a biophysical basis for disease, Biopolymers 66 (2002) 350–358.
[66] C. Kubisch, B.C. Schroeder, T. Friedrich, B. Lutjohann, A. El-Amraoui, S. Marlin, C. Petit, T.J. Jentsch, KCNQ4, a novel potassium channel expressed in sensory outer hair cells, is mutated in dominant deafness, Cell 96 (1999) 437–446.
[67] M.C. Sanguinetti, M.E. Curran, A. Zou, J. Shen, P.S. Spector, D.L. Atkinson, M.T. Keating, Coassembly of K(V)LQT1 and minK (IsK) proteins to form cardiac I(Ks) potassium channel, Nature 384 (1996) 80–83.
[68] J. Barhanin, F. Lesage, E. Guillemare, M. Fink, M. Lazdunski, G. Romey, K(V)LQT1 and lsK (minK) proteins associate to form the I(Ks) cardiac potassium current, Nature 384 (1996) 78–80.
[69] L.P. Lai, C.L. Deng, A.J. Moss, R.S. Kass, C.S. Liang, Polymorphism of the gene encoding a human minimal potassium ion channel (minK), Gene 151 (1994) 339–340.
[70] L.P. Lai, M.J. Su, H.M. Yeh, J.L. Lin, F.T. Chiang, J.J. Hwang, K.L. Hsu, C.D. Tseng, W.P. Lien, Y.Z. Tseng, S.K. Huang, Association of the human minK gene 38G allele with atrial fibrillation: evidence of possible genetic control on the pathogenesis of atrial fibrillation, Am. Heart J. 144 (2002) 485–490.
[71] N. Patil, D.R. Cox, D. Bhat, M. Faham, R.M. Myers, A.S. Peterson, A potassium channel mutation in weaver mice implicates membrane excitability in granule cell differentiation, Nat. Genet. 11 (1995) 126–129.
[72] Fei Li, Hongyan Li, Lihong Hu, Miufan Kwan, Guanhua Chen, Qing-Yu He, Hongzhe Sun, Structure, assembly, and topology of the G185R mutant of the fourth transmembrane domain of divalent metal transporter, J. Am. Chem. Soc. 127 (2005) 1414–1423.
[73] S.J. Opella, F.M. Marassi, J.J. Gesell, A.P. Valente, Y. Kim, M. Oblatt-Montal, M. Montal, Structures of the M2 channel-lining segments from nicotinic acetylcholine and NMDA receptors by NMR spectroscopy, Nat. Struct. Biol. (1999) 374–379.
[74] A. Schulz, K. Bruns, P. Henklein, G. Krause, M. Schubert, T. Gudermann, V. Wray, G. Schultz, Schöneberg, Requirement of specific intrahelical interactions for stabilizing the inactive conformation of glycoprotein hormone receptors, J. Biol. Chem. 275 (2000) 37860–37869.
[75] K.R. MacKenzie, J.H. Prestegard, D.M. Engelman, A transmembrane helix dimer: structure and implications, Science 276 (1997) 131–133.
[76] Michael A. Massiah, Young-Hee Ko, Peter L. Pedersen, Albert S. Mildvan, Cystic fibrosis transmembrane conductance regulator: solution structures of peptides based on the Phe508 region, the most common site of disease-causing ¢F508 mutation, Biochemistry 38 (1999) 7453–7461.
[77] Mei Y. Choi, Anthony W. Partridge, Craig Daniels, Kai Du, Gergely L. Lukacs, Charles M. Deber, Destabilization of the transmembrane domain induces misfolding in a phenotypic mutant of cystic fibrosis transmembrane conductance regulator, J. Biol. Chem. 280 (2005) 4968–4974.
[78] A.G. Therien, C.M. Deber, Oligomerization of a peptide derived from the transmembrane region of the sodium pump gamma subunit: effect of the pathological mutation G41R, J. Mol. Biol. 322 (2002) 583–590.
[79] M.L. Plotkowski, S. Kim, M.L. Phillips, A.W. Partridge, C.M. Deber, J.U. Bowie, Transmembrane domain of myelin protein zero can form dimers: possible implications for myelin construction, Biochemistry 46 (2007) 12164–12173.